

# NATURAL CONVECTIVE HEAT TRANSFER FROM A VERTICAL ISOTHERMAL SURFACE TO A NON-NEWTONIAN SUTTERBY FLUID

**TETSU FUJII, OSAMU MIYATAKE, MOTOO FUJII, HIROSHI TANAKA and KENTARO MURAKAMI**  
 Research Institute of Industrial Science, Kyushu University, Fukuoka-812, Japan

(Received 25 April 1973)

**Abstract**—This paper deals with the laminar natural convection of a non-Newtonian fluid along a vertical isothermal surface. The boundary-layer equations for a Sutterby fluid are solved numerically, and several characteristics of the non-similarity solution are represented graphically. An approximate expression of local Nusselt number  $Nu_x$  is proposed as

$$Nu_x = 0.50 (Gr_{0x} Pr_0)^{0.25(1+m)},$$

where

$$m = 0.04 Pr_0^{-0.23} A^{3.7} Pr_0^{-0.14} Z_0^{0.63} A^{0.46},$$

$Gr_{0x}$  and  $Pr_0$  are Grashof number and Prandtl number based on zero viscosity respectively, and  $A$  and  $Z_0$  are non-Newtonian parameters.

Local heat-transfer coefficients are obtained by experiments with aqueous solutions of polyethylene-oxide (PEO) and carboxymethylcellulose (CMC). The experimental results are in excellent agreement with the theoretical ones.

## NOMENCLATURE

- |  |  |
|--|--|
| <p><math>A, B</math>, constants in the Sutterby model (6)<br/> <math>[-]</math>, <math>[s]</math>;</p> <p><math>F'(\eta)</math>, dimensionless velocity component in <math>x</math>-direction defined by (34);</p> <p><math>Gr_{nx}</math>, generalized Grashof number for a power law fluid defined by (35);</p> <p><math>Gr_{0x}</math>, Grashof number for a Sutterby fluid defined by (22);</p> <p><math>Gr_x</math>, Grashof number for a Newtonian fluid;</p> <p><math>g</math>, gravitational acceleration <math>[m/s^2]</math>;</p> <p><math>K</math>, constant in the power law model (37)<br/> <math>[Ns^n/m^2]</math>;</p> <p><math>l</math>, height of the heated surface <math>[m]</math>;</p> <p><math>Nu_x</math>, local Nusselt number defined by (21);</p> <p><math>n</math>, constant in the power law model (37);</p> <p><math>Pr_{nx}</math>, generalized Prandtl number for a power law fluid defined by (36);</p> <p><math>Pr_0</math>, Prandtl number for a Sutterby fluid defined by (13);</p> | <p><math>Pr</math>, Prandtl number for a Newtonian fluid;</p> <p><math>R</math>, viscosity ratio defined by (14);</p> <p><math>T</math>, temperature <math>[^\circ C]</math>;</p> <p><math>U, V</math>, dimensionless velocity components in <math>X</math>- and <math>Y</math>-directions defined by (9) and (10) respectively;</p> <p><math>u, v</math>, velocity components in <math>x</math>- and <math>y</math>-directions respectively <math>[m/s]</math>;</p> <p><math>X, Y</math>, dimensionless coordinates for <math>x</math> and <math>y</math> defined by (7) and (8) respectively;</p> <p><math>x</math>, vertical distance from the leading edge of the heated surface <math>[m]</math>;</p> <p><math>y</math>, distance normally away from the heated surface <math>[m]</math>;</p> <p><math>Z_0</math>, dimensionless parameter defined by (12).</p> <p>Greek symbols</p> <p><math>\alpha_x</math>, local heat-transfer coefficient based on <math>(T_w - T_\infty)</math> <math>[W/m^2 \text{ deg}]</math>;</p> |
|--|--|

- $\beta$ , average coefficient of thermal expansion [1/deg];  
 $\dot{\gamma}$ , shear rate [1/s];  
 $\eta$ , similarity variable defined by (32);  
 $\theta$ , dimensionless temperature defined by (11);  
 $\kappa$ , thermal diffusivity [m<sup>2</sup>/s];  
 $\lambda$ , thermal conductivity [W/m deg];  
 $\mu$ , dynamic viscosity of a Newtonian fluid [Ns/m<sup>2</sup>];  
 $\mu_{app}$ , apparent dynamic viscosity expressed by (6) or (37) [Ns/m<sup>2</sup>];  
 $\mu_0$ , constant in the Sutterby model (6) (zero viscosity) [Ns/m<sup>2</sup>];  
 $\nu_0$ , kinematic zero viscosity =  $\mu_0/\rho$  [m<sup>2</sup>/s];  
 $\rho$ , density [kg/m<sup>3</sup>].

#### Subscripts

- $x$ , local values at  $x$ ;  
 $w$ , values at the heated surface;  
 $\infty$ , values in the ambient fluid.

### 1. INTRODUCTION

SEVERAL informations are available on the natural convective heat transfer from a vertical isothermal surface to a non-Newtonian fluid. Acrivos [1] and Akagi [2] obtained similarity solutions for a power law fluid. Tien [3] and Tien-Tsuei [4] obtained approximate solutions by using the integral method for a power law fluid and a Ellis fluid respectively. In all of these analyses the inertia term in the momentum equation is ignored. The shear rate induced in natural convection is comparatively small and varies in the directions both parallel and perpendicular to the heated surface. The purely viscous non-Newtonian behavior in the shear rate range of interest is not accurately described by the power law model which has two constants, but by the Ellis [5] or the Sutterby model [6] which has three constants. The existence of the similarity solution of the boundary-layer equations is intimately connected with the use of the power law model and the neglect of the inertia term in the momentum equation. There-

fore, the natural convection of non-Newtonian fluid possesses inherently no similarity.

As for experimental studies, Reilly *et al.* [7] and Sharma-Adelman [8] obtained average heat-transfer coefficients by using aqueous solutions of carboxypolyethylene. Although their results are more or less different from the similarity solution for the power law model [1], it is impossible to examine the discrepancy in detail, since there is no assurance of the heated plates used being really isothermal. The propriety of theoretical studies may be proved well when more detailed measurements are carried out on the local heat-transfer coefficient.

The object of the present study is to obtain an accurate solution of the boundary-layer equations and to compare it with the experimental results for the case of the natural convective heat transfer from a vertical isothermal surface to a purely viscous non-Newtonian fluid.

### 2. BASIC EQUATIONS

The pertinent equations of the boundary layer are given as

$$\frac{\partial u}{\partial x} + \frac{\partial v}{\partial y} = 0, \quad (1)$$

$$u \frac{\partial u}{\partial x} + v \frac{\partial u}{\partial y} = g\beta(T - T_\infty) + \frac{1}{\rho} \frac{\partial}{\partial y} \left( \mu_{app} \frac{\partial u}{\partial y} \right), \quad (2)$$

$$u \frac{\partial T}{\partial x} + v \frac{\partial T}{\partial y} = \kappa \frac{\partial^2 T}{\partial y^2}, \quad (3)$$

with boundary conditions of

$$u = v = 0, T = T_w \quad \text{at } y = 0, \quad (4)$$

$$u = 0, \quad T = T_\infty \quad \text{at } y = \infty. \quad (5)$$

where  $x$  is the vertical distance from the leading edge of the heated surface,  $y$  the distance normally away from the heated surface,  $u$  and  $v$  velocity components in  $x$ - and  $y$ -directions respectively, and  $T$  temperature. Average coefficient of thermal expansion  $\beta$ , density  $\rho$ , apparent viscosity  $\mu_{app}$  and thermal diffusivity  $\kappa$  may be evaluated at each appropriate reference temperature.

Apparent viscosity  $\mu_{app}$  of the Sutterby model is given as

$$\mu_{app} = \mu_0 \left( \frac{\text{arc sinh } B\dot{\gamma}}{B\dot{\gamma}} \right)^A, \quad (6)$$

where  $A$ ,  $B$  and  $\mu_0$  are constants and  $\dot{\gamma}$  is shear rate. This expression characterizes well the non-Newtonian behavior of fluids of dispersion system such as high polymer solutions over a wide range of shear rate.

By using the following dimensionless quantities

$$X = \frac{x}{(Bv_0)^{\frac{1}{2}}}, \quad (7)$$

$$Y = \frac{y}{(Bv_0)^{\frac{1}{2}}} Z_0^{\frac{1}{2}} Pr_0^{\frac{1}{2}}, \quad (8)$$

$$U = \frac{u Pr_0^{\frac{1}{2}}}{\{(Bv_0)^{\frac{1}{2}} g \beta (T_w - T_\infty)\}^{\frac{1}{2}}}, \quad (9)$$

$$V = \frac{v Z_0^{\frac{1}{2}} Pr_0^{\frac{1}{2}}}{\{(Bv_0)^{\frac{1}{2}} g \beta (T_w - T_\infty)\}^{\frac{1}{2}}}, \quad (10)$$

$$\Theta = \frac{T - T_\infty}{T_w - T_\infty}, \quad (11)$$

$$Z_0 = \frac{(Bv_0)^{\frac{1}{2}} g \beta (T_w - T_\infty)}{v_0^2}, \quad (12)$$

$$Pr_0 = \frac{v_0}{\kappa}, \quad (13)$$

$$R = \frac{\mu_{app}}{\mu_0}, \quad (14)$$

(1)–(5) are transformed as

$$\frac{\partial U}{\partial X} + \frac{\partial V}{\partial Y} = 0, \quad (15)$$

$$\frac{1}{Pr_0} \left( U \frac{\partial U}{\partial X} + V \frac{\partial U}{\partial Y} \right) = \Theta + \frac{\partial}{\partial Y} \left( R \frac{\partial U}{\partial Y} \right), \quad (16)$$

$$U \frac{\partial \Theta}{\partial X} + V \frac{\partial \Theta}{\partial Y} = \frac{\partial^2 \Theta}{\partial Y^2}, \quad (17)$$

$$U = V = 0, \quad \Theta = 1 \quad \text{at } Y = 0, \quad (18)$$

$$U = 0, \quad \Theta = 0 \quad \text{at } Y = \infty. \quad (19)$$

$B\dot{\gamma}$  in  $R$  is written as

$$B\dot{\gamma} = B \frac{\partial u}{\partial y} = Z_0^{\frac{1}{2}} Pr_0^{-\frac{1}{2}} \frac{\partial U}{\partial Y}, \quad (20)$$

Local Nusselt number  $Nu_x$  is given by

$$Nu_x = \frac{\alpha_w x}{\lambda} = \frac{-(\partial T / \partial y)_w x}{T_w - T_\infty} = X (Z_0 Pr_0)^{\frac{1}{2}} \left( -\frac{\partial \Theta}{\partial Y} \right)_w \quad (21)$$

$$= X^{\frac{1}{2}} (Gr_{0x} Pr_0)^{\frac{1}{2}} \left( -\frac{\partial \Theta}{\partial Y} \right)_w,$$

where local Grashof number  $Gr_{0x}$  is defined by

$$Gr_{0x} = \frac{g \beta (T_w - T_\infty) x^3}{v_0^2}. \quad (22)$$

It is seen from (15)–(21) that  $Nu_x$  for a Sutterby fluid is a function of  $Gr_{0x} Pr_0$ ,  $Pr_0$ ,  $A$  and  $Z_0$ , though that for a Newtonian fluid is a function of  $Gr_x Pr$  and  $Pr$ , that is, the former has two more parameters than the latter. Therefore, the effect of temperature difference  $(T_w - T_\infty)$  on  $Nu_x$  is not represented only by Grashof number, unlike the case of Newtonian fluid, since  $(T_w - T_\infty)$  is included also in  $Z_0$ .

In the above transformations  $(Bv_0)^{\frac{1}{2}}$  is introduced as the unit of length. When the height of the heated surface  $l$  is introduced instead, as done in the most of previous analyses, there remains a surplus parameter  $(Bv_0)^{\frac{1}{2}}/l$  in the expression of local Nusselt number. This surplus parameter not only makes calculation more complicated, but also gives a superficial appearance as if the height  $l$  affects on the local values in the boundary layer.

### 3. NUMERICAL SOLUTION

Equations (15)–(17) are relaxed to finite difference form, and solved numerically by a

forward-marching, implicit method with iteration. Equation (15) is relaxed as

$$\frac{U_{m+1,n} - U_{m,n} + U_{m+1,n-1} - U_{m,n-1}}{2\Delta X} + \frac{V_{m+1,n} - V_{m+1,n-1}}{\Delta Y} = 0, \quad (23)$$

and each term of (16) and (17) is written as

$$U \partial U / \partial X = U_{m+1,n}^0 (U_{m+1,n} - U_{m,n}) / \Delta X, \quad (24)$$

$$U \partial \Theta / \partial X = U_{m+1,n}^0 (\Theta_{m+1,n} - \Theta_{m,n}) / \Delta X, \quad (25)$$

$$V \partial U / \partial Y = V_{m+1,n}^0 (U_{m+1,n+1} - U_{m+1,n-1}) / 2\Delta Y, \quad (26)$$

$$V \partial \Theta / \partial Y = V_{m+1,n}^0 (\Theta_{m+1,n+1} - \Theta_{m+1,n-1}) / 2\Delta Y, \quad (27)$$

$$\partial^2 \Theta / \partial Y^2 = (\Theta_{m+1,n+1} - 2\Theta_{m+1,n} + \Theta_{m+1,n-1}) / (\Delta Y)^2, \quad (28)$$

$$\begin{aligned} \partial(R \partial U / \partial Y) / \partial Y &= R_{m+1,n}^0 (U_{m+1,n+1} - 2U_{m+1,n} + U_{m+1,n-1}) / (\Delta Y)^2 \\ &+ (R_{m+1,n+1}^0 - R_{m+1,n-1}^0) (U_{m+1,n+1} - U_{m+1,n-1}) / (2\Delta Y)^2, \end{aligned} \quad (29)$$

$$\Theta = \Theta_{m+1,n}^0 \text{ (in the momentum equation),} \quad (30)$$

where  $(m + 1)$  and  $n$  represent the  $X$  and  $Y$

points of the nodal points, and superscript  $0$  represents the value obtained in the preceding iteration on  $(m + 1)$  level. The local Nusselt number is calculated from

$$Nu_x = X^{1/2} (Gr_{0,x} Pr_0)^{1/4} \times \left( \frac{3 - 4\Theta_{m+1,2} + \Theta_{m+1,3}}{2\Delta Y} \right). \quad (31)$$

Details of the computation are described in [9].

First, the computation was made on a Newtonian fluid of  $A = 0$ ,  $Pr_0 = 100$  to test the accuracy of the method. The obtained local Nusselt number showed good agreement with the similarity solution of Ostrach [10] for  $Pr = 100$  within the accuracy of 2.5 per cent for  $Gr_x Pr > 10^6$ .

The profiles of temperature and vertical velocity component for the case of  $A = 0.5$ .  $Z_0 = 184$  and  $Pr_0 = 100$  are compared with the similarity solutions for the power law model by Acrivos [1], Akagi [2] and Tien [3] in Fig. 1. Abscissa  $\eta$  and ordinates  $\Theta(\eta)$  and  $F'(\eta)$  in the figure are the similarity variable and the dimensionless temperature and velocity component defined by Akagi respectively, that is,

$$\eta = \left( \frac{n}{3n + 1} \right)^{n/(3n+1)} \left( \frac{y}{x} \right) (Gr_{nx} Pr_{nx}^n)^{1/(3n+1)}, \quad (32)$$

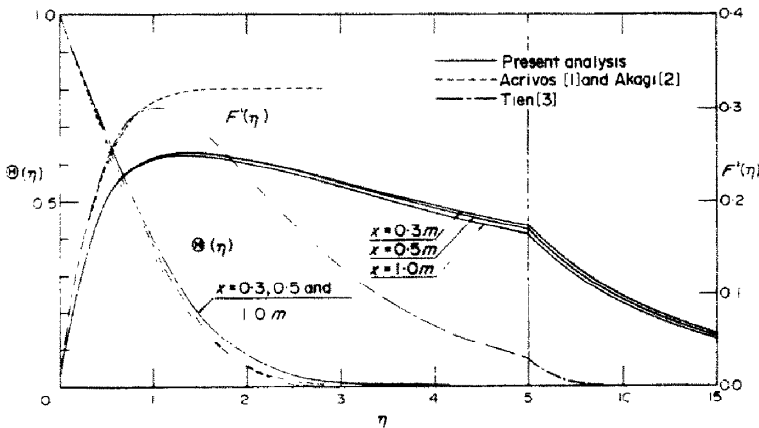


FIG. 1. Comparison of profiles of temperature and vertical component.

Table 1. Comparison of local Nusselt numbers

Case	$\dot{\gamma}$ (1/s)	n	K (Ns <sup>n</sup> /m <sup>2</sup> )	Nu <sub>x</sub> at x = 0.5 m		
				Acrivos [1] and Akagi [2]	Tien [3]	Present analysis
1	1.528	0.646	0.337 × 10 <sup>-2</sup>	183.9	183.1	
2	15.28	0.587	0.894 × 10 <sup>-2</sup>	139.2	137.6	130.2
3	152.8	0.562	0.262 × 10 <sup>-1</sup>	95.6	94.2	

$$\Theta(\eta) = \frac{T - T_\infty}{T_w - T_\infty} \tag{33}$$

$$F'(\eta) = u x^{n/(2-n)} Pr_{nx}^{(n+1)/(3n+1)} \times \left(\frac{3n+1}{n}\right)^{(n+1)/(3n+1)} \times \left(\frac{K}{\rho}\right)^{n/(3n+1)} \times Gr_{nx}^{2/(3n+1)} \tag{34}$$

where  $Gr_{nx}$  and  $Pr_{nx}$  are the generalized Grashof and Prandtl numbers defined by

$$Gr_{nx} = g\beta(T_w - T_\infty) x^{(2+n)/(2-n)} \left(\frac{K}{\rho}\right)^{2/(2-n)} \tag{35}$$

$$Pr_{nx} = \frac{1}{\kappa} \left(\frac{K}{\rho}\right)^{1/(2-n)} x^{(2-2n)/(2-n)} \tag{36}$$

respectively.  $K$  and  $n$  in (32)–(36) are constants in the power law model

$$\mu_{app} = K |\dot{\gamma}|^{n-1} \tag{37}$$

When  $B = 10s$ ,  $\mu_0 = 1.5 \times 10^{-2}$  Ns/m<sup>2</sup> and  $\rho = 10^3$  kg/m<sup>3</sup> are given to the present solution,

profiles of  $u, v, T$  and  $\dot{\gamma}$  are reckoned. The value of  $n$  evaluated from these data, however, varies from 0.598 to 0.584 and correspondingly  $K$  from  $8.7 \times 10^{-3}$  to  $9.5 \times 10^{-3}$  Ns<sup>n</sup>/m<sup>2</sup> on the heated surface within the range of  $x = 0.1$ – $1$  m. Therefore,  $n = 0.588$  and  $K = 8.94 \times 10^{-3}$  Ns<sup>n</sup>/m<sup>2</sup> at  $x = 0.5$  m are taken as reference values. By using these values, the present solution is converted and plotted in Fig. 1.

The discrepancy due to the choice of non-Newtonian model is salient for the profile of vertical velocity component, but it is slight for the temperature profile as shown in Fig. 1. Accordingly, as far as the heat-transfer coefficient is concerned, the power law model may be applied, provided that the decision of  $n$  and  $K$  is made at the shear rate on the heated surface in its midheight. The propriety of this recommendation is shown in Table 1. Case 2 in the table corresponds to the case where  $n$  and  $K$  are decided at  $\dot{\gamma} = 15.28$  s<sup>-1</sup> on the heated surface at  $x = 0.5$  m as aforementioned, and cases 1

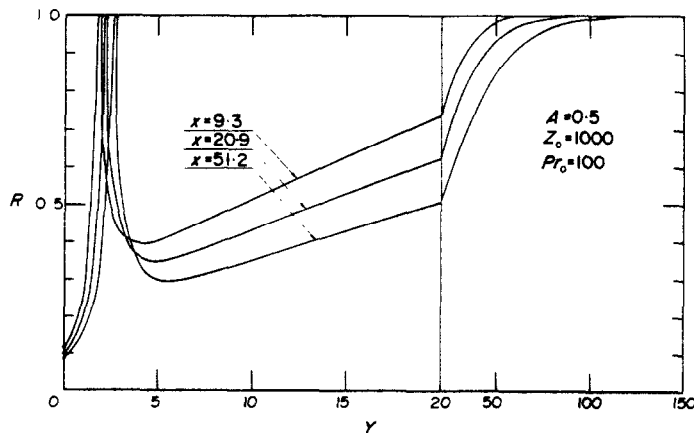


FIG. 2. Profiles of apparent viscosity.

and 3 correspond to those at  $\dot{\gamma} = 1.528$  and  $152.8 \text{ s}^{-1}$  respectively. Though the results on case 2 are in good agreement with the present solution, cases 1 and 3 give largely different results.

An example of the profiles of  $R$  is shown in Fig. 2. In the region near the heated surface where the shear rate is large,  $R$  decreases considerably. At the point where  $U$  attains its peak,  $R$  becomes unity, i.e.  $\mu_{\text{app}} = \mu_0$ , because of the extinction of the shear rate. Since gradient  $\partial U/\partial Y$  is rather gradual in the outer boundary

layer, the decrease of  $R$  is not so large as in the inner boundary layer, and  $R$  gradually approaches to unity again at a great distance from the surface. With the development of the boundary layer, the extent of lowering of  $R$  increases and the effect of the non-Newtonian property gradually becomes predominant.

The effects of  $A$ ,  $Z_0$  and  $Pr_0$  on the relation of  $Nu_x$  vs  $Gr_{0x}Pr_0$  are shown in Figs. 3(a)–(c) respectively. Generally,  $Nu_x$  for the non-Newtonian fluid is higher than that for the Newtonian fluid of  $\nu = \nu_0$ . Since the increases of  $A$  and  $Z_0$  make non-Newtonian property large,  $Nu_x$  increases with them as shown in Figs. 3(a) and (b). The difference of  $Nu_x$  between non-Newtonian and Newtonian fluids becomes large with the decrease of Prandtl number as shown in Fig. 3(c). Such a result is caused by the fact that the smaller  $Pr_0$  is, the larger the induced shear rate becomes, which enhances the decrease of the apparent viscosity near the heated surface.

By the modification of the relation of  $Nu_x$  vs  $Gr_x Pr$  for a Newtonian fluid of large Prandtl number, numerical results are correlated approximately as

$$Nu_x = 0.50(Gr_{0x}Pr_0)^{0.25(1+m)} \quad (38)$$

where

$$m = 0.04Pr_0^{-0.23}A^{3.7}Pr_0^{-0.34}Z_0^{0.63}A^{0.66} \quad (39)$$

Expression (38) predicts the local Nusselt number within the accuracy of  $\pm 10$  per cent in the range of  $A = 0-1$ ,  $Z_0 = 0-10^3$ ,  $Pr_0 = 10^2-3 \times 10^3$  and  $Gr_{0x}Pr_0 = 10^6-10^{11}$ . The comparison of exponent  $m$  in (38) with theoretical values evaluated at  $Gr_{0x}Pr_0 = 6 \times 10^8$  for  $Pr_0 = 1000$  is shown in Fig. 4.

#### 4. EXPERIMENTS

Aqueous solutions of 0.2 and 0.5% polyethyleneoxide (PEO) and 2.0% carboxymethylcellulose(CMC) were used as non-Newtonian fluids. Since PEO solution exhibits the non-Newtonian behavior to the range of low shear rate and reduces to a Newtonian fluid, i.e.

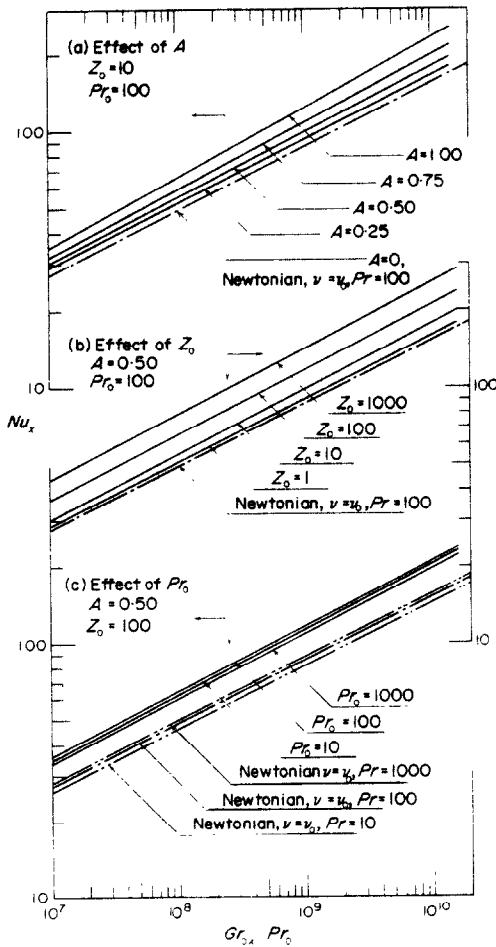


FIG. 3. Variation of local Nusselt number with the product of local Grashof number and Prandtl number. (a) effect of  $A$ . (b) effect of  $Z_0$ . (c) effect of  $Pr_0$ .

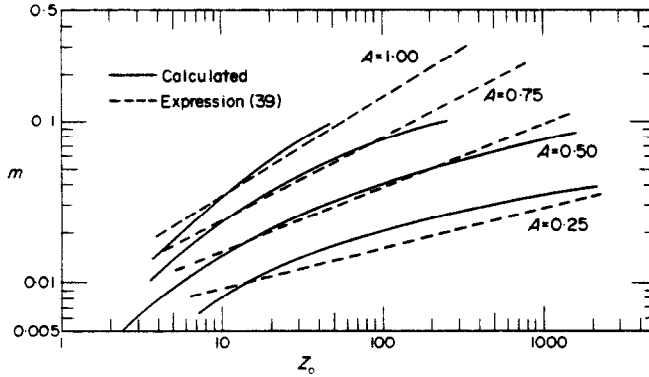


FIG. 4. Comparison of exponent  $m$  of (39) with calculated values.

$\mu_{app} = \mu_0$ , at a lower shear rate with the increase of its concentration, it is considered to serve for verifying numerical calculations when experiments are performed with fluids of various concentrations. CMC solution is often used in the experimental study of forced convection of a non-Newtonian fluid. This solution fails, however, to exhibit the non-Newtonian behavior at such a comparatively low shear rate as induced under the natural convection, since it reduces to a Newtonian fluid at a moderate shear rate. Accordingly, the heat-transfer characteristics of CMC solution are considered

to be little different from those of a Newtonian fluid. In order to confirm this fact experimentally CMC solution was used.

The measured relation between the apparent viscosity  $\mu_{app}$  and the shear rate  $\dot{\gamma}$  for each fluid is shown in Fig. 5. Such vent curves of PEO solutions cannot be represented by the power law model but accurately by the Sutterby model. In the figure are also shown the ranges of shear rate induced in the present experiments of natural convection at the heated surface from 0.1 to 1 m height. By the way, the Maron-Krieger-Sisko viscometer [11] and a co-axial

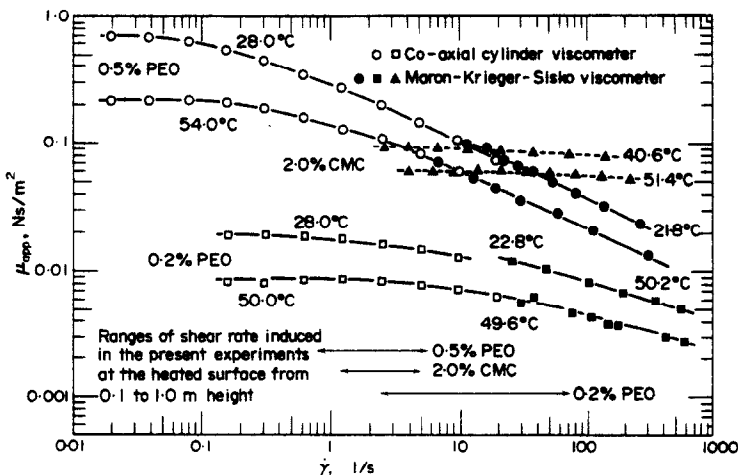


FIG. 5. Variation of apparent viscosity with shear rate.

cylinder viscometer were used for the ranges of higher and lower shear rate respectively. The viscometry by the former was carried out at four temperature levels in a range of 20–60°C but only two of them are shown in the figure. The constants in the Sutterby model  $A$ ,  $B$  and  $\mu_0$  were determined by overlapping these obtained curves on the master plots of Fig. 6.

into 20 parts corresponding to 20 unit heaters. The temperature of ambient fluid  $T_\infty$  was measured vertically at 14 points. The deviation of the measured values of  $T_w$  from the average one was within  $\pm 2.5$  per cent of the average temperature difference of  $(T_w - T_\infty)$ , and the gradient of stratified temperature of ambient fluid was at most 5°C/m. The ambient fluid was

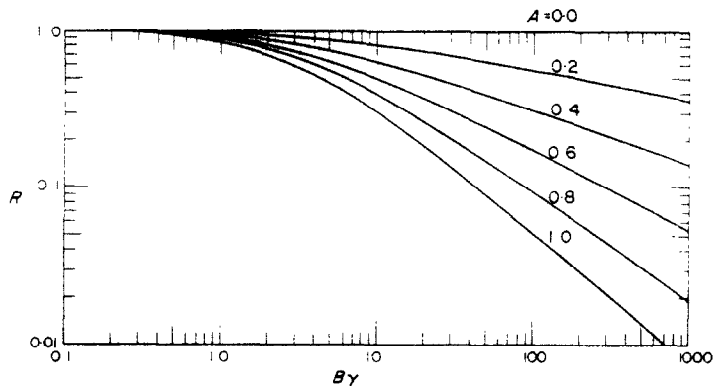


FIG. 6. Master plots of the Sutterby model.

The apparatus and procedure of experiments of natural convection were the same as those described in [12]. A vertical brass cylinder of 82.0 mm o.d. and 1.00 m height was immersed in a container of 385 mm i.d. and 1.42 m height. The cylinder was heated from inside by 20 electric heaters, and the electric input to each unit heater was regulated so as to make the surface temperature uniform and was measured by a voltmeter and an ammeter. The local surface temperature  $T_w$  was measured by using the thermocouples at 20 points in the center of each section of the cylinder which was subdivided

sampled before and after each test run of about 2 hr, and from its viscometric data the degradation of fluid was confirmed to be negligibly small during a series of test runs.

The effect of the curvature of the heated cylinder upon the local Nusselt number was estimated to be negligibly small from the theoretical analysis of a Newtonian fluid [13]. The mean heat flux of a unit heater was assumed as the local heat flux in the center of each section in the calculation of local Nusselt number. The physical properties of fluids, except for the model constants, were assumed as the

Table 2. Conditions of experiments

Run	Symbol	Fluid	$T_w$ (°C)	$T_\infty$ (°C)	$A$	$Z_0$	$Pr_0$
1	○	0.2% PEO	27.3	17.1	0.3	10	150
2	□	0.2% PEO	36.2	16.5	0.3	24	120
3	△	0.2% PEO	63.5	28.6	0.3	110	50
4	●	0.5% PEO	44.1	22.0	0.4	170	2900
5	■	0.5% PEO	63.8	22.3	0.4	500	1500
6	×	2.0% CMC	39.5	20.2	0.5	0.008	800
7	+	2.0% CMC	56.1	21.2	0.5	0.025	490



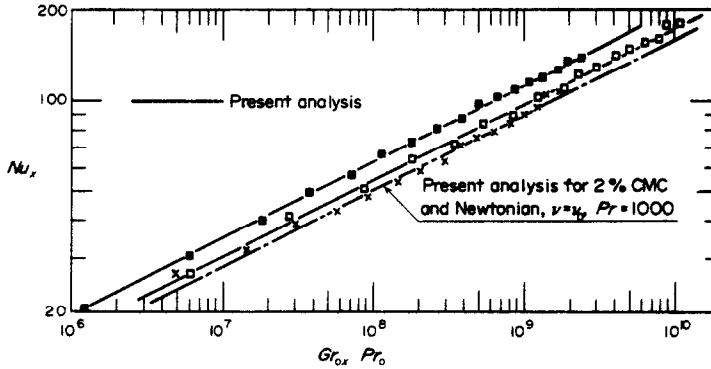


FIG. 7. Comparison between experimental results and present analysis. Symbols correspond to those in Table 2.

same as those of pure water [14, 15]. The coefficient of thermal expansion  $\beta$  was taken as the average one evaluated in the temperature range from  $T_\infty$  to  $(T_w - T_\infty)/2$ . The other physical properties together with model constant  $\mu_0$  were evaluated at reference temperature  $T_w - 0.25(T_w - T_\infty)$ . The variation of model constants  $A$  and  $B$  with temperature was negligibly small. The experimental conditions are shown in Table 2.

A comparison between the experimental results and the present analysis is shown in Fig. 7. The excellent agreement between them verifies the propriety of the present analysis. In the case of CMC solution both the measured values and the theoretical lines come close to the theoretical line of a Newtonian fluid as expected

before. The approximate expression (38) is also in good agreement with the measured values within the accuracy of  $\pm 10$  per cent as shown in Fig. 8.

5. CONCLUSIONS

- (1) The Sutterby model is applied to the analysis of natural convection of a pure viscous non-Newtonian fluid.
- (2) The height of the heated surface must not be used as the characteristic length in the dimensionless transformation, since the boundary layer of non-Newtonian fluid possesses no similarity.
- (3) The profiles of temperature and vertical velocity component are calculated with sufficient accuracy by taking account of the inertia term

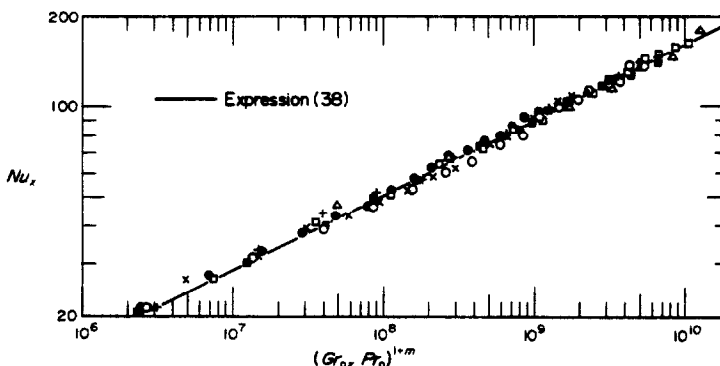


FIG. 8. Comparison between experimental results and approximate expression (38). Symbols correspond to those in Table 2.

in the momentum equation. The profile of the latter is greatly different from the existing results of analysis for the power law model.

(4) With the development of the boundary layer, the extent of lowering of apparent viscosity increases and the effect of the non-Newtonian property gradually becomes predominant.

(5) The effects of  $Pr_0$  and non-Newtonian parameters  $A$  and  $Z_0$  on the relation of  $Nu_x$  vs  $Gr_{0x}Pr_0$  are obtained. The effect of temperature difference ( $T_w - T_\infty$ ) on  $Nu_x$  cannot be appreciated by Grashof number only, unlike the case of a Newtonian fluid.

(6) The experimental results of  $Nu_x$  are in excellent agreement with the present numerical analysis, and they are in agreement with approximate expression (38) within  $\pm 10$  per cent. The heat-transfer coefficient of CMC solution did not show any non-Newtonian characteristics in the present experiments.

#### ACKNOWLEDGEMENT

The numerical computation of difference equations and the processing of experimental data were performed with the digital computer FACOM-230-60 in Computer Center, Kyushu University.

#### REFERENCES

1. A. ACRIVOS, A theoretical analysis of laminar natural convection heat transfer to non-Newtonian fluids, *A.I.Ch.E. Jl.* **6**, 584-590 (1960).
2. S. AKAGI, Free convection heat transfer of non-Newtonian fluid (in Japanese), *Trans. Japan Soc. Mech. Engrs* **32**, 919-929 (1966).
3. C. TIEN, Laminar natural convection heat transfer from vertical plate to power law fluid, *Appl. Sci. Res.* **17** 233-248 (1967).
4. C. TIEN and H. S. TSUEI, Laminar natural convection heat transfer in Ellis fluids, *Appl. Sci. Res.* **20**, 131-147 (1969).
5. J. C. SLATTERY and R. B. BIRD, Non-newtonian flow past a sphere, *Chem. Engng Sci.* **16**, 231-241 (1961).
6. J. L. SUTTERBY, Laminar converging flow of dilute polymer solutions in conical section—I. Viscosity data, new viscosity model, tube flow solution, *A.I.Ch.E. Jl* **12**, 63-68 (1966).
7. I. G. REILLY, C. TIEN and M. ADELMAN, Experimental study of natural convection heat transfer from a vertical plate in a non-Newtonian fluid, *Can. J. Chem. Engng* **43**, 157-160 (1965).
8. K. K. SHARMA and M. ADELMAN, Experimental study of natural convection heat transfer from a vertical plate in a non-Newtonian fluid, *Can. J. Chem. Engng* **47**, 553-555 (1969).
9. T. FUJII, O. MIYATAKE, M. FUJII and H. TANAKA, A numerical analysis of natural convection heat transfer to non-Newtonian Sutterby fluids (in Japanese), *Trans. Japan Soc. Mech. Engrs* **38**, 2883-2890 (1972).
10. S. OSTRACH, An analysis of laminar free-convection flow and heat transfer about a flat plate parallel to the direction of the generating body force, NACA Tech. Rep. 1111 (1953).
11. S. H. MARON, I. M. KRIEGER and A. W. SISCO, A capillary viscometer with continuously varying pressure head, *J. Appl. Phys.* **25**, 971-976 (1954).
12. T. FUJII, M. TAKEUCHI, M. FUJII, K. SUZAKI and H. UEHARA, Experiments on natural-convection heat transfer from the outer surface of a vertical cylinder to liquids, *Int. J. Heat Mass Transfer* **13**, 753-787 (1970).
13. T. FUJII and H. UEHARA, Laminar natural-convective heat transfer from the outer surface of a vertical cylinder, *Int. J. Heat Mass Transfer* **13**, 607-615 (1970).
14. N. E. DORSEY, *Properties of Ordinary Water-Substance*, p. 22. Reinhold, New York (1940).
15. *VDI, Wärmeatlas*, Dbl. VDI-Verlag, Düsseldorf (1953).

#### CONVECTION NATURELLE D'UN FLUIDE NON-NEWTONIEN DE SUTTERBY AU VOISINAGE D'UNE SURFACE VERTICALE ISOTHERME

**Résumé**—Cet article traite de la convection laminaire naturelle d'un fluide non-newtonien le long d'une surface verticale et isotherme. Les équations de la couche limite pour un fluide de Sutterby sont résolues numériquement et plusieurs caractéristiques de la solution non similaire sont représentées graphiquement. On propose une expression approchée du nombre de Nusselt local :

$$Nu_x = 0,50(Gr_{0x}Pr_0)^{0,25(1+m)}$$

où

$$m = 0,04 Pr_0^{-0,23} A^{3,7} Pr_0^{-0,34} Z_0^{0,63} A^{0,66}$$

$Gr_{0x}$  et  $Pr_0$  sont respectivement le nombre de Grashof et le nombre de Prandtl,  $A$  et  $Z_0$  sont les paramètres non-newtoniens.

Le coefficient de transfert thermique local est obtenu expérimentalement avec des solutions aqueuses d'oxyde de polyéthylène (PEO) et de carboxyméthylcellulose (CMC). Les résultats expérimentaux et théoriques sont en excellent accord.

### WÄRMEÜBERGANG DURCH FREIE KONVEKTION VON EINER SENKRECHTEN ISOTHERMEN FLÄCHE AN EINE NICHT-NEWTONISCHE SUTTERBY-FLÜSSIGKEIT

**Zusammenfassung**—Diese Arbeit behandelt die laminare freie Konvektion einer nicht-Newtonischen Flüssigkeit längs einer senkrechten isothermen Fläche. Die Grenzschichtgleichungen für die Sutterby-Flüssigkeit werden numerisch gelöst und einige Charakteristika der nichtähnlichen Lösung werden graphisch dargestellt. Für die örtliche Nussel-Zahl  $Nu_x$  wird ein Näherungsausdruck vorgeschlagen:

$$Nu_x = 0,5(Gr_{0x}Pr_0)^{0,25(1+m)}$$

mit

$$m = 0,04 Pr_0^{-0,23} A^{3,7} \cdot Pr_0^{0,34} \cdot Z_0^{0,63} A^{0,66}$$

$Gr_{0x}$  und  $Pr_0$  sind die mit der Nullviskosität gebildeten Grashof- bzw. Prandtl-Zahlen,  $A$  und  $Z_0$  sind nicht-Newtonische Parameter.

Örtliche Wärmeübergangskoeffizienten werden erhalten aus Experimenten mit wässrigen Lösungen von Polyäthylenoxid (PEO) und Carboxymethylcellulose (CMC). Die experimentellen Ergebnisse stimmen hervorragend mit den theoretischen überein.

### СВОБОДНОКОНВЕКТИВНЫЙ ПЕРЕНОС ТЕПЛА ОТ ВЕРТИКАЛЬНОЙ ИЗОТЕРМИЧЕСКОЙ ПОВЕРХНОСТИ К НЕНЬЮТОНОВСКОЙ ЖИДКОСТИ

**Аннотация**—В работе приведено исследование естественной конвекции при ламинарном обтекании вертикальной изотермической поверхности неньютоновской жидкостью. Уравнения пограничного слоя для жидкости Саттерби решены численно, а некоторые характеристики неавтономного решения рассчитаны графически. Предложено приближенное выражение для локального числа Нуссельта следующего вида:

$$Nu_x = 0,50(Gr_{0x}Pr_0)^{0,25(1+m)},$$

где

$$m = 0,04 Pr_0^{-0,23} A^{3,7} Pr_0^{-0,37} Z_0^{0,63} A^{0,66}$$

$Gr_{0x}$  и  $Pr_0$ —соответственно числа Грасгофа и Прандтля, рассчитанные при нулевой вязкости, а  $A$ ,  $Z_0$ —параметры неньютоновской жидкости.

Коэффициенты локального теплообмена получены в экспериментах с водными растворами полиэтиленоксида (ПЭО) и карбоксиметилцеллюлозы (КМЦ). Результаты эксперимента хорошо согласуются с теоретическими расчетами.